CHAPTER II

REVIEW OF THE RELATED LITERATURES

## 1. The limb development

### A. Early stages of limb development

The limb buds first appear as elevations of the ventrolateral body wall toward the end of the fourth week. Limb development begins with the activation of a group of mesenchymal cells in the lateral mesoderm. Homeobox-containing (*HOX*) genes regulate patterning in vertebrate limb development. The limb buds from deep to a thick band of ectoderm. The upper limb buds are visible by day 26 or 27, and the lower limb buds appear a day or two later. Each limb bud consists of a mass of mesenchyme is derived from the somatic layer of lateral mesoderm. The limb buds elongate by the proliferation of the mesenchyme. The upper limb buds appear disproportionately low on the embryo's trunk because of the early development of the cranial half of the embryo. The early stage of limb development are alike for the upper and lower limb; however development of the upper limb buds precedes that of the lower limb buds by about 2 days. In addition, there are distinct differences between the development of the hand and foot because of their form and function. The upper limb buds develop opposite the caudal cervical segments, and the lower limb buds from opposite the lumbar and upper sacral segments.

At the apex of each limb buds the ectoderm thickens to form an apical ectodermal ridge (AER). The AER, a multi layered epithelial structure, interacts with mesenchyme in the limb bud, promoting outgrowth of the limb bud. Expression of endogenous fibroblast growth factors (*FGFs*) in the AER is involved in this process. The AER exerts an inductive influence on the limb mesenchyme that initiates growth and development of the limbs in a proximal-distal axis. Mesenchymal cells aggregate at the posterior margin of the limb bud to form the zone of polarizing activity (ZPA). Fibroblast

growth factors from the AER activate the ZPA, which causes expression of the sonic hedgehog gene (*Shh*). Experimental studies show that *Shh* secretions control the patterning of the limb along the anterior-posterior axis. Expression of Wnt7 from dorsal epidermis of the limb bud and engrailed-1 (*EN-1*) from the ventral aspect are involved in specifying the dorsal-ventral axis. Of interest, the AER itself is maintained by inductive signals from *Shh* and *Wnt7*. The mesenchyme adjacent to the AER consists of undifferentiated, rapidly proliferating cells, whereas mesenchymal cells proximal to it differentiate into blood vessels and cartilage bone models. Expression of homeobox genes is essential for the normal patterning of the limbs. The distal ends of the flipper-like limb buds flatten into paddle-like hand and foot plates. Experimental studies have also shown that endogenous retinoic acid is involved in limb development and patterning formation.

By the end of the sixth week, mesenchymal tissue in the hand plates has condensed to form digital rays. These mesenchymal condensation outline the pattern of the digits (fingers). During the seventh week, similar condensations of mesenchyme form digital rays and toe buds in the foot plates. At the tip of the digital rays, apart of the AER induces development of the mesenchyme into mesenchymal primodia of the bones (phalanges) in the digits. The intervals between the digit rays are occupied by loose mesenchyme. Soon the intervening regions of mesenchyme break down, forming notches between the digital rays. As the tissue break down progresses, separate digits are formed by the end of the eight week. Programmed cell death (apoptosis) is responsible for the tissue break down in the interdigital regions and it is probably mediated by bone morphogenetic proteins (*BMPs*), signaling molecules of the *TGFß* superfamily. Blocking these cellular and molecular events could account for syndactyly, webbing or fusion of the fingers or toes (*7, 8, 9*).

## B. Final stages of limb development

As the limbs elongate during the fifth week, mesenchymal models of the bones are formed by cellular aggregrations. Chondrification centers appear later in the fifth week. By the end of the sixth week, the entire limb skeleton is cartilaginous.

Osteogenesis of long bones begins in the seventh week from primary ossification centers in the middle of the cartilaginous models of the long bones. Primary ossification centers are present in all long bones by the twelfth week. Ossification of the carpal (wrist) bones begins during the first year after birth.

As the long bone form, myoblasts aggregate and form a large muscle mass in each limb bud. In general this muscle mass separates into dorsal (extensor) and ventral (flexor) components. The mesenchyme in the limb bud gives rise to bones, ligaments, and blood vessels. From the dermomyotome regions of the somites, myogenic precursor cells also migrate into the limb bud and later differentiate to myoblasts – precursors of muscle cells. The cervical and lumbosarcral myotomes contribute to the muscles of the pectoral and pelvic girdles, respectively.

## 2. Mesomelic dysplasia, Kantaputra type

Mesomelic dysplasia, Kantaputra type (MDK) (OMIM *156232) is classified as osteochondrodysplasia was documented in a three-generation Thai family (Fig.1). To date, there are 12 types of mesomelic dysplasia as previously described (*10, 11, 12, 13*). However, only 3 types of mesomelic dysplasia consisting Dyschondrosteosis (Leri-Weill), Langer type and recessive Robinow type were reported that resulted from mutation in *SHOX* gene (Leri-Weill and Langer type) and mutation in *ROR2* gene, respectively.

### Clinical features

MDK is an autosomal dominant disorder, characterized by bilateral severe shortening of the ulnae and shortening and bowing of the radii (Fig. 2 and 3). The fibula

is hypoplastic in most patients (Fig. 4). Synostosis is observed between tibia and fibula, and the malformed calcaneus and talus. The fibula prominence is a constant feature (Fig.6). Carpal and tarsal synostoses are present in some affected people. However, the pattern does not appear to be consistent (*14*). The affected patients stand on the tip of their toes (Fig. 5).
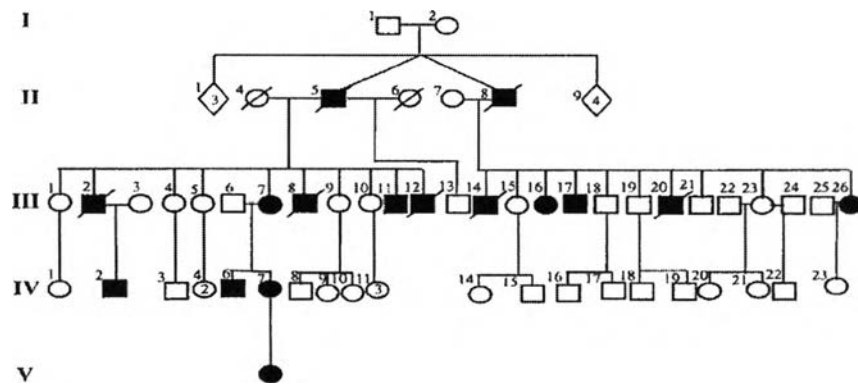


Figure 1. Pedigree of a Thai family



Figure 2. a–c: Patient IV2 at ages 8, 15, and 21, respectively. d: Front row from left to right. Patients IV7, IV2, V1, III7, and Kantaputra.
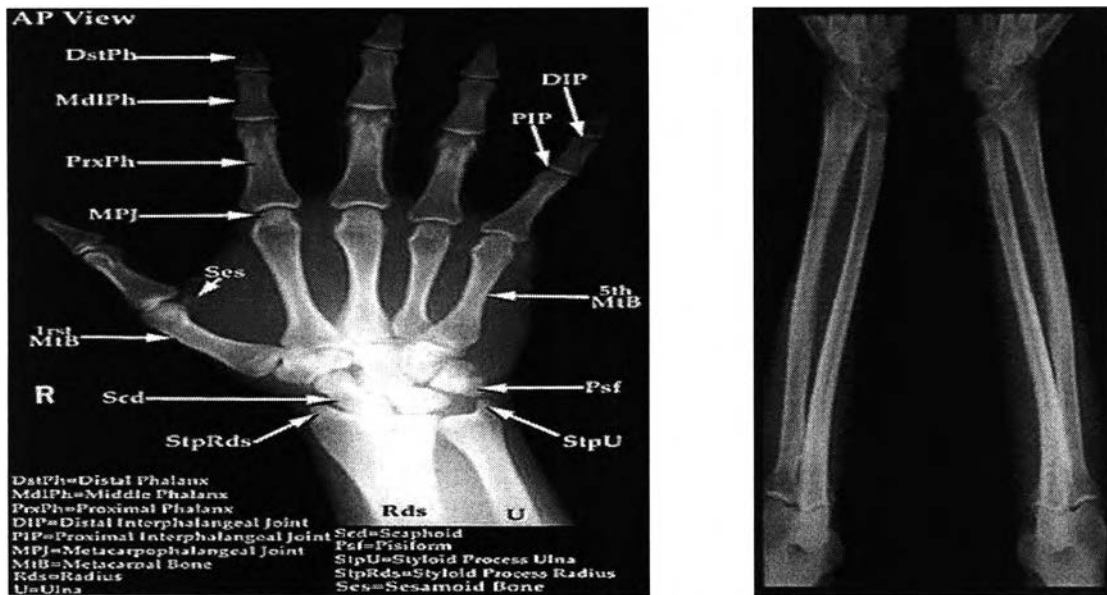
Figure 3. Arm radiographs of normal and MDK patient. Upper row; normal hand and arm. Lower row; right arms of patient at (a) age 8 and (b) 21 years. Left arms at (c) age 8 and (d) age 21 years. Note progressively bowed radii, large distal humeri, and overlapped carpal bones. Flexion contracture of the distal interphalangeal joints of 4 and 5 on both sides.

Figure 4. Foot and ankle radiographs. Normal right foot (a) and (b). Patient's right foot at (c) age 8 and (d) age 21 years. Malformed talus is fused with fibula at age 8 years. Calcaneus is missing. Tibia-talus-fibular synostosis and overlapped tarsal bones · narrow spaces between them at age 21. Note distal symphalangism at toe 5 at age 21.



Figure 5. Tip toe standing on the dorsal of Patients (a) and (b) V1. d: IV2. e: III7. Ballerina-like standing of Patients (c) III2, (f) III17, and (g) III11
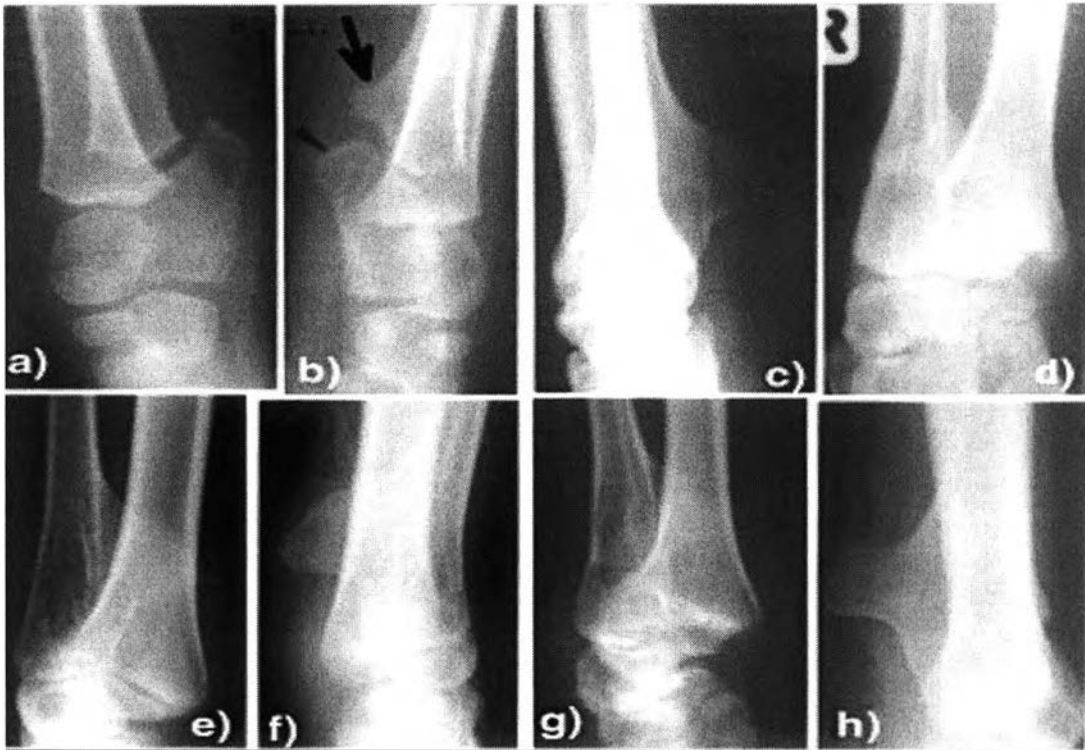
Figure 6. Ankle radiographs of (a) Patient V1. Right ankle. Note vertical positioned calcaneus. No fibular prominence. b: Patient V1. Left ankle. Note fibular prominence (arrow). Malformed and separate calcaneus (arrow head). Fibular prominences in Patients (c) IV2, (d) IV7, (e) IV6, (f) III11, (g) III7, (h) III17.

## 3. The studies of MDK

With reference to the breakpoints of a balanced translocation [t(2;8)(q31;p21)] in patients from previously reported Italian family with skeletal dysplasia that appears similar to MDK (3), positional candidate gene approach using linkage analysis was performed in the Thai family using 50 CA-repeat markers mapped to nearby region (2q22-q34 and 8p24-p21) of the translocation breakpoints. The result clearly ruled out a linkage of MDK to marker loci at the 8p24-p21 region, whereas all nine affected members available for the study shared a haplotype at four loci (D2S2284, D2S326, D2S2188, and D2S2314) spanning about 22.7 cM in the 2q24-q32 region. The computer

assisted two-point linkage analysis revealed maximum logarithm of odd (lod) scores of 4.82, 4.21, 4.82, and 4.21 at these loci, respectively. These data indicated that the MDK locus is in the vicinity of *D2S2284* and *D2S2188* loci that are most likely mapped to 2q24-q32. Based on evidences from *Drosophila*, mouse model and human, they proposed that HOXD genes, especially those located at the 5' region of the *HOXD* cluster, were strong candidates for the gene responsible for the MDK phenotype.

Another report of MDK were found in three generation of a Dutch family (*2*), which a grandmother had skeletal abnormalities consisting of a short stature, bilateral symmetry very short, broad and bowed radii, very short and broad ulna, mildly short lower legs, short proximal end fibula, abnormal ankles, abnormal calcaneus and talus and pes equines. They had normal craniofacial features, normal intelligence and normal chromosome. They concluded that this skeletal dysplasia resembles the autosomal dominant mesomelic dysplasia, Kantaputra type. *SHOX* mutation screening and haplotype analysis are then performed. Using DHPLC (Denaturation high performance liquid chromatography) and MLPA (Mutiplex-ligation dependent probe amplification) for detection of point mutation and large genomic rearrangement, no mutation or rearrangement could be detected making involvement of *SHOX* very unlikely. From VNTR marker analysis using markers that have been shown linkage with MDK locus, they observed perfect co-segregation with disease phenotype. Nevertheless, their family was too small to obtain a significant LOD score. They thought it was very likely that the mesomelic dysplasia in their family was of the Kantaputra type.

However, Kantaputra comment that although there were similarities between Thai and Dutch patients, but some were not (*14*). In upper extremities, the ulnae and radii of Thai patients were more severely affected, showing more shortening and the radii were more severely bowed. The arrangement of the carpal bones in all Thai adult patients was more disorganized with narrow spaces among them or more fusion between them. In lower extremities, more severely affected tibiae, ballerina-like standing, and fibular prominence were presented only in Thai patients. Kantaputra

believed the syndrome in the Dutch family was unique and deserved its own distinct entity. However, he convinced that the syndrome was allelic to MDK.

## 4. Limb malformation and the Human *HOX* genes

*HOX* genes encode a family of transcription factors of fundamental importance for body patterning during embryonic development (*15*). Human ,like most vertebrates, have 39 *HOX* genes organized into four clusters, named *HOXA*, *HOXB*, *HOXC*, *HOXD*, located on chromosomes 7p14, 17q21, 12q13, and 2q31, respectively. The major roles are in the development of the central nervous system, axial skeleton, gastrointestinal and urogenital tracts, external genitalia, and limbs. The first two limb malformations shown to be caused by mutation in the human *HOX* genes were synpolydactyly and hand-foot-genital syndrome, which result from mutations in *HOXD13* and *HOXA13*, respectively. The *HOXD10* gene mutations causing M319K were found in a family with isolated Congenital Vertical Talus (CVT) and Charcot-Marie-Tooth disease (*5*). Moreover, deletion form *HOXD3-HOXD13* caused monodactylous limbs and abnormal genitalia (*16*).

## 5. Mutations in the other type of mesomelic dysplasia

In Mesomelic dyplasia, Langer type (OMIM 249700) and Leri-weill dyschondrosteosis (OMIM127300), *SHOX* mutations were reported as the cause of these diseases, whereas *ROR2* mutation is reported in recessive Robinow type (OMIM 268310). *SHOX* gene and *ROR2* gene are located at Xpter-p22.32 and 9q22, respectively (*10*). The disease-causing mechanism of other types of mesomelic dysplasia are still to be discovered.

## 6. The clues for MDK

### A. With a reference from an Italian family with mesomelic dysplasia

Spitz et al. (2002) report the cloning of the breakpoints of a human t(2;8)(q31;p21) balanced translocation associated with mesomelic dysplasia of the upper limb as well as with the vertebral defects. They shown that this translocation did not disrupt any gene, hence it mostly exerted its deleterious effect by modifying gene regulation. Although it can not be ruled out that break point in chromosome 8 might not be the cause, they hypothesized, based on several lines of evidence, that the breakpoint of chromosome 2 disrupted the regulatory region and resulted in a misregulation of some or all *HOXD* genes. It is known that some regulatory traits of *HOX* genes are controlled by sequences localized at a distance from the complex. Several studies have suggested that the expression of *HOXD* genes in the zeugopod (medial part of the limbs) is under the control of a shared enhancer sequence, which may be localized outside the complex (*17*). Sugawara et al (2002) also cloned the breakpoints and found the same result. In addition, they found that 2q31 breakpoint was mapped within the linkage interval of the MDK family (*18*).

### B. The mouse models

Double homozygous mutant (*Hoxa11 -/-, Hoxd11 -/-*) mice caused by targeted disruption showed an almost absence of radius and ulna (Fig. 7). Moreover, tibia and fibula were also malformed and proximal tarsal bones are also missing. Notably, the zeugopod (ulna and radius) was more affected than the autopod (hand and digit) (*19*). Moreover, the double mutant mice also resulted in reduction of the *fgf8* and *fgf10* expression and caused developmental arrest (*20, 21*).
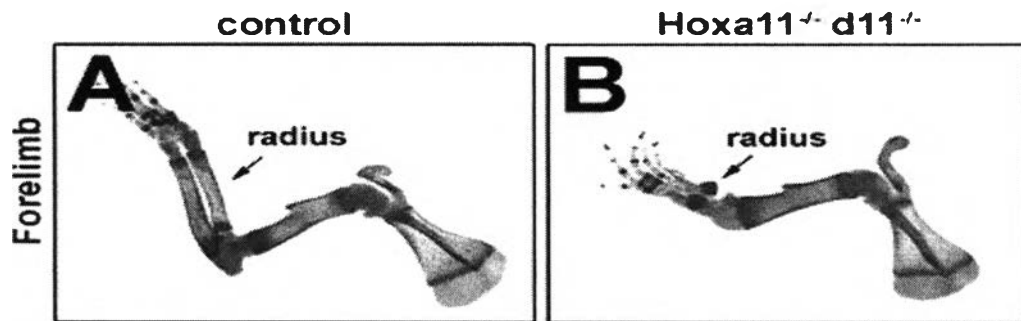
**control**   **Hoxa11⁻ᐟ⁻ d11⁻ᐟ⁻**

Figure 7 The forelimb phenotype in (A) control and (B) double homozygous mutant mice

*Ulnaless* (*Ul*), an X-ray-induced dominant mutation in mice, severely disrupts development of forearms and forelegs. The mutation mapped on chromosome 2, tightly linked to the *HoxD* complex, a cluster of regulatory genes required for proper morphogenesis. In particular, 5' located (posterior) *Hoxd* genes are involved in limb development and combined mutations within these genes result in severe alterations in appendicular skeleton. They indicated that Ulnaless was allelic to *Hoxd* genes and suggested that *Ul* is a regulatory mutation that interfered with a control mechanism shared by multiple genes to coordinate *Hoxd* function during limb morphogenesis. In addition, heterozygous mice (*Ul/+*) showed a phenotype resembling MDK consisting shortening of ulna and shortening and bowing of radii (Fig. 8) (*22*).
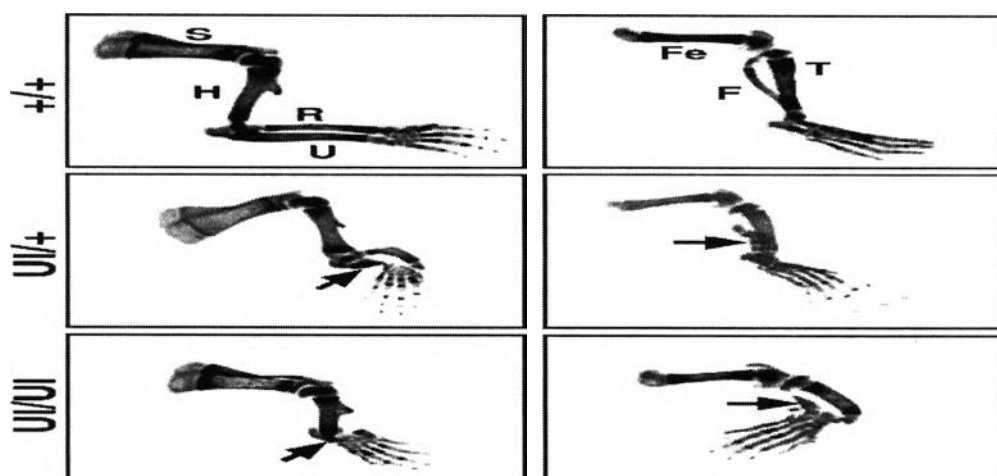


Figure 8 The forelimb (left column) and hindlimb (right column) phenotype of wild type, heterozygous mutant and homozygous mutant mice.

It was proposed that ulnaless mutation alters a cis-acting element that regulates *HoxD* expression specifically in the appendicular axes of the embryo based on the evidences of deregulation of 5' *HoxD* gene expression in Ulnaless limb buds. In addition, deregulation of *Hoxa11* was also observed (*23*).

Using a targeted enhancer-trap approach and DNA sequence comparisons of suspected region among human, mouse, and puffer fish an unusual interspecies conservation in that region, later called global control region (GCR), which was capable of controlling transcription of several genes was discovered. They finally found that ulnaless mice was caused by balanced inversion that modified the topography of the locus which centromeric breakpoint was within *Lnp* (centomeric to *Evx2* and *HoxD* cluster), while telomeric breakpoint was 770 kb away form centromeric breakpoint (downstream of *Mtx2* gene) (Fig. 9) (*24*).
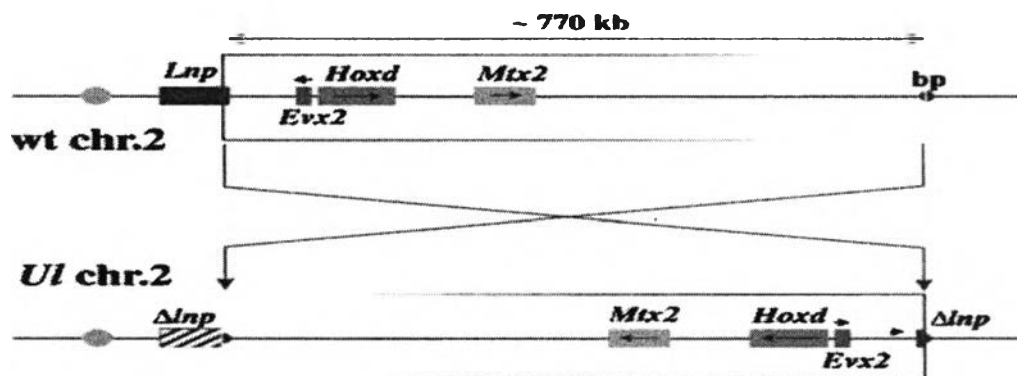


Figure 9 A balanced paracentric inversion in *Ulnaless* mice

The developmental regulation of vertebrate *Hox* gene transcription relies on the interplay between local and long-range control. To study this complex genomic organization, the large chromosomal rearrangements *in vivo* was induced. A large 7-cM inversion was engineered, which split the *Hoxd* cluster into two independent pieces. Expression analyses showed a partition of global enhancer, allowing for their precise

topographic allocation on either side of the cluster. It indicated that expression of *Hox* genes in these distinct domains is controlled by different mechanisms (*25, 26, 27*).

The supporting data, integrated form multiple systematic strategies, indicated that a temporal and spatial collinearity of the *HoxD* cluster and the nearby genes are controlled by opposite site of regulatory region consisting centromeric GCR and telomeric ELCR (Early limb control region) (*28, 29, 30, 31, 32*).
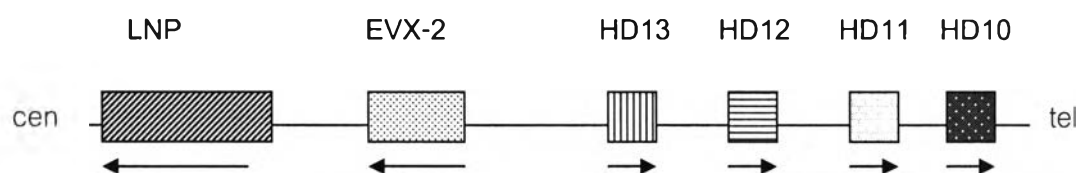
## 7. The candidate genes



**Figure 10** The orientation of candidate genes within 2q31 region.

### *LNP* (Lunarpark, KIAA1715)

The *Lunapark* gene was found by study of ESTs. It mapped to 2q31-q32. This gene contains 13 exons.The gene size is about 76.6 kb and transcript is about 5.76 kb which encode 428 amino acids. It has orthologous counterparts in plants, fungi, animals such as *C. elegans, Drosophila* and vertebrates. Some part of a *LNP* protein was hypothesized as a transmembrane domain. Because of the presence, in both vertebrates and arthropods, of the peptide LNPARK, it was named " LUNAPARK ". *LNP* expresses in blood, bone, bone marrow, brain, connective tissue, liver, pancreas, adrenal gland, parathyroid, placenta, eye, embryonic tissue, cervix, ovary, uterus, prostate, testis, bladder, kidney, tongue, larynx, heart, lymph node, thymus, mammary gland, muscle, lung, trachea, skin, vascular, colon, stomach, nerve tissue,embryo,

juvenile (< 17 years old), adult (> 17 years old),adrenal tumor, chondrosarcoma, glioma, non-glioma, breast (mammary gland) cancer, colorectal tumor, gastrointestinal tumor, germ cell tumor, cervical tumor, laryngeal cancer, oral tumor, kidney tumor, leukemia, liver tumor, ovarian tumor, pancreatic tumor, respiratory tract tumor, skin tumor, soft tissue/muscle tissue tumor, urinary bladder tumor, normal, non-neoplasia

### EVX2 (Even-skipped homeobox 2)

The *EVX-2* gene was first studied in *Drosophila* embryogenesis. In human, it was mapped to 2q31-q32 and found that it contained 4 exons. It encodes homeodomains which might involve in a process of segmentation and a morphogenesis of vertebrate limbs (*33*). The size of transcript and protein are 2.18 kb and 727 amino acids, respectively.

### The posterior HOXD genes

On the basis of spatial and temporal expression, the 3'*HOXD*, like *HOXD1*, are generally expressed early in anterior and proximal regions, whereas genes at the 5' end, like *HOXD10* to *HOXD13* are expressed later. Then *HOXD10-HOXD13* genes were called as posterior *HOXD* genes. All *HOX* proteins bind specific DNA sequences via a highly conserved 60 amino acid DNA-binding motif called the homeodomain. This is encoded by 180-bp sequence element called the homeobox, which in all *HOX* genes is located in the second of the two coding exons.

### HOXD11

This gene also mapped to 2q31 and the gene size is 2.23 kb containg 2 exons. The transcript is 658 bp which encodes 338 amino acids. The *NUP98-HOXD11* fusion transcript was the cause of acute myelomonocytic leukaemia. It expresses in **bone, brain, cervix, kidney, placenta, prostate, uterus** in both embryonic and adult stages.

## HOXD10

This gene consists of 2 coding exons in a 2.92 kb genomic DNA region. The transcript is 1.55 kb which encodes 340 amino acid. It expresses in colon, kidney, ovary, prostate, soft tissue, uterus in both embryonic and adult stage. It was reported that mutation in this gene cause CMT and CVT diseases.

## 8. Relative Quantification

The two most commonly used methods to analyze data from real-time, quantitative PCR experiment are absolute quantification and relative quantification. Absolute quantification determines the input copy number, usually by relating the PCR signal to a standard curve. Relative quantification relates the PCR signal of the target transcript in a case to that of another sample such as an unrelated control. The $2^{-\Delta\Delta C_t}$ method is a convenient way to analyze the relative changes in gene expression for realtime quantitative PCR experiments ($34, 35$).

First of all, the $\Delta C_t$ value for each sample is determined by calculating the differences between $C_t$ value of the target gene and $C_t$ value of the endogenous reference gene. This is determined for each unknown sample as well as for the calibrator sample.

$\Delta C_t$ (sample) = $C_t$ target gene - $C_t$ reference gene

$\Delta C_t$ (calibrator) = $C_t$ target gene - $C_t$ reference gene

Next, the $\Delta\Delta C_t$ value for each sample is determined by subtracting the $\Delta C_t$ value of the calibrator from the $\Delta C_t$ value of the sample.

$\Delta\Delta C_t$ = $\Delta C_t$ (sample) - $\Delta C_t$ (calibrator)

IF the PCR efficiencies of the target gene and endogenous reference gene are comparable, the normalized level of target gene expression is calculated by using the formula:

**Normalized target gene expression level in sample** $= 2^{-\Delta\Delta_{Ct}}$